

Effect of Smartphone Light Fluxes on Cornea: A Biophysical Study

P. M. Dongre, Vinod D. Jaiswal, Suraj Singh

Department of Biophysics, University of Mumbai, Mumbai, Maharashtra, India

Abstract

Objective: Biophysical study to investigate (a) the effects of smartphone light fluxes (SPLF) on isolated mammalian cornea and model protein (insulin), (b) to predict the possible visual interference of SPLF. **Materials and Methods:** Fresh goat cornea and insulin protein were used as an experimental model system. The energy of absorbed SPLF was measured using chemical dosimeter. The effect of SPLF on the aggregation of model protein was studied using fluorescence spectroscopy and dynamic light scattering (DLS). Fluorescence microscopy, scanning electron microscopy (SEM), DLS, were used for cornea imaging. **Results:** The spectral emission peak of SPLF was observed at 380 nm and 420 nm. Absorbed radiation of SPLF was found to be 2.82 mWm^{-2} and 1.92 mWm^{-2} for collimated (focussed) and noncollimated (nonfocussed) condition, respectively. Secondary structural changes of insulin were observed by fluorescence and zeta potential after SPLF exposure. SEM study revealed the disorganization of the epithelial cell surface, increase in intercellular space, disorganization of primary epithelium layer, and exposure of the second layer is seen in depth. Differential Interference Microscopy showed an optical gradient in images that appears to be changed in specimen structure. Fluorescence microscopy showed disorganization in epithelial cell pattern. A significant difference in bio-molecular permeation was observed in the exposed cornea. Ultraviolet UV-visible spectroscopy study indicated a reduction in light transmission through the cornea. **Conclusions:** The obtained results indicate changes in physicochemical and morphological modifications in the cornea and insulin modifications after exposed to SPLF.

Keywords: Cornea disorganization, protein aggregation, smartphone light fluxes

Received on: 07-10-2019

Review completed on: 09-07-2020

Accepted on: 06-08-2020

Published on: 13-10-2020

INTRODUCTION

Smartphones and other modern devices emit a high-frequency electromagnetic radiation; there is a strong rationale for evaluating the adverse effects of microwave radiation and the Smartphone light fluxes (SPLF) of smartphone on health. An ample research data are available on the adverse effect of microwave radiation from mobile phone on health,^[1-3] however, unfortunately, there are no scientific data available on the effect of SPLF on eyes and visual apparatus. The smartphone screens are the formulation of aluminum silicate that is made up of aluminum, silicon, oxygen. Various other forms of displays are thin film register technology-liquid crystal display (LCD), in-pace-switching-LCD, organic light-emitting diode, etc. These light sources possess blue-enriched light that could have detrimental effects on the human eye when observed very closely. A portion of blue light overlaps with high energy ultraviolet (UV) radiation. UV exposure is known to cause skin cancers, accelerated skin

aging, cataract of the eye lens, and another eye disease.^[4-11] However, UV-induced biological effects depend on the energy of radiation emitted. This involves the absorption of a single photon by the molecules and the production of the excited state in which electron of the absorbing molecule is released at high-energy level.^[12] The primary product of UV is generally reactive species or free radicals, which can produce effects that can last for hours, days, or even years. DNA is the most critical targets for damage. Similarly, cell death, chromosome changes, mutation, and morphological transformation were observed after UV exposure in prokaryotic and eukaryotic cells.^[13,14]

Address for correspondence: Dr. P. M. Dongre,
Department of Biophysics, University of Mumbai, Santacruz (E),
Mumbai - 400 098, Maharashtra, India.
E-mail: drpmdongre@yahoo.co.in

Access this article online

Quick Response Code:



Website:
www.jmp.org.in

DOI:
10.4103/jmp.JMP_89_19

This is an open access journal, and articles are distributed under the terms of the Creative Commons Attribution-NonCommercial-ShareAlike 4.0 License, which allows others to remix, tweak, and build upon the work non-commercially, as long as appropriate credit is given and the new creations are licensed under the identical terms.

For reprints contact: reprints@medknow.com

How to cite this article: Dongre PM, Jaiswal VD, Singh S. Effect of smartphone light fluxes on cornea: A biophysical study. *J Med Phys* 2020;45:187-94.

Cornea covers the front portion of the eye and its chief function is to refract light and focus most of it that enter eyes. The cornea is mainly composed of protein and cells.^[15,16] The cornea is the first line of exposure organ of the eye. UV can penetrate through the cornea, and even reach the anterior portion of the lens. An epidemiological study reported that UVR contributes multiple factors of eye disease, including pterygium, photokeratitis, climatic droplet keratopathy (CDK) and ocular surface squamous neoplasia, etc.^[17] Chronic UV exposure to the cornea is associated with spheroidal degeneration such as Bietti corneal degeneration, Labrador keratopathy, Eskimo corneal degeneration, etc.^[18]

In this study, we analyzed the effect of SPLF exposure on model protein insulin and mammalian cornea using various biophysical tools. Here we report the changes in structures, physicochemical, morphological changes in cornea/epithelial cells, and protein after exposure to SPLF.

MATERIALS AND METHODS

Potassium chloride, Calcium chloride, Fluorescein dye (SD fine chemicals), Sodium bicarbonate, Sodium chloride (Himedia), Ascorbic Acid (Loba chemicals), Insulin, Human recombinant (Sigma Aldrich) were used for the study.

Ultraviolet dosimetry (actinometry)

Actinometry was performed to estimate the amount of absorbed SPLF energy.^[19-21] Potassium ferric oxalate crystals ($K_3[Fe(C_2O_4)_3]$, 0.006 M) were dissolved in 0.1 N H_2SO_4 solution. Crystals being UV sensitive, entire experiment was performed in dark. 10 ml solution was transferred in Petri-dish (area 38.5 cm^2). The exposure distance was kept 15 cm from SPLF [Figure 1a and b]. The solution was exposed for different time intervals with constant stirring. 1 ml irradiated sample of each interval was removed and transferred to a solvent containing 0.1 N H_2SO_4 (9 ml), CH_3COONa buffer (5 ml, pH 3.5), distilled water (3 ml) and o-phenanthroline indicator (2 ml). The solution was incubated for 30 min. The resulting $Fe(Phen)_3^{+2}$ orange color complex was measured at 510 nm. The amount of SPLF energy absorbed was estimated using equation 1.

$$\text{Energy absorbed (erg / sec.cm}^2\text{)} = \frac{\text{No. of molecule of } Fe^{+2} \times h \times c}{\phi \times t \times A \times \lambda} \quad (1)$$

where h = plank's constant, c = velocity of light, λ = wavelength of light (366 nm), A = area of Petri plate (38.5 cm^2), t = time of irradiation, ϕ = quantum yield (1.22).

Insulin study

Insulin (0.2 mg/ml) was prepared using 20% acetic acid (pH = 2) and filtered with $0.22\ \mu$ syringe filter. Insulin was exposed with SPLF for 1 h (energy) at room temperature for any structural changes, and appropriate control was kept in dark. Observations were recorded for triplicates.

Fluorescent measurements (Varian) were recorded with 10 mm path length rectangular quartz cuvette in the emission wavelength range of 280–500 nm. The excitation wavelength was set to 276 nm. The excitation and emission slit width was set to 5 nm with the PMT voltage of 650 V. Resonance light scattering (RLS) measurements were performed using a synchronous mode. The excitation and the emission monochromators were scanned simultaneously in the wavelength range of 200–700 nm. $\Delta\lambda$ -0 nm, Excitation and emission slit widths - 2.5 nm and PMT voltage-450 V were additional parameters.

Time-resolved fluorescence measurements were performed to understand the effect of the SPLF on insulin protein. Diode laser-based time-correlated single-photon counting spectrometer (TCSPC, IBH, U.K.) was used for time-resolved fluorescence measurement using excitation light-emitting diode source (276 nm). The emitted photon was detected using PMT detector.

Zeta potential measurement (Malvern ZS90) was employed to understand the stability of the SPLF exposed insulin molecules. The samples were analyzed using the dip cell DTS1070 at 298 K, with an average run of 3. The wavelength of laser light used for the measurement is 632.8 nm, with a scattering angle of 90°C .

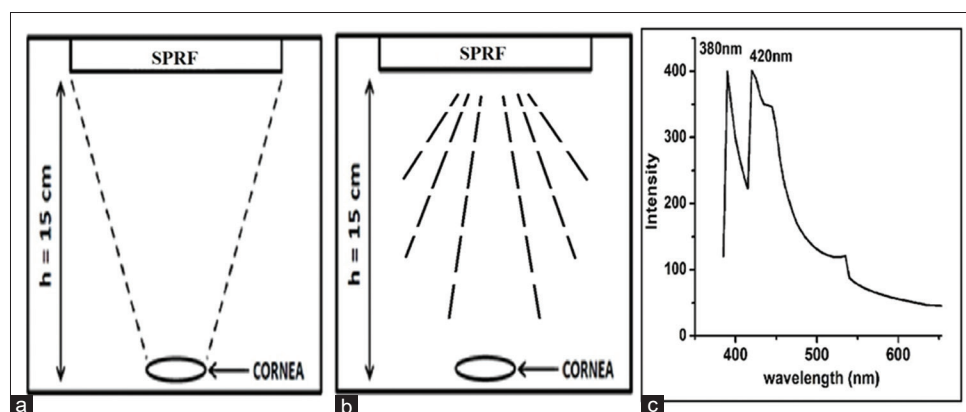


Figure 1: (a) Schematic diagram of the exposure unit-collimation of smartphone light fluxes and (b) noncollimation smart phone light fluxes; (c) spectral measurement of smartphone light fluxes

Cornea study

Preparation of cornea

Fresh goat (age 7–9 months) eyeballs were obtained from the slaughterhouse and preserved in chilled ringer solution. Eyeballs were further processed, excised into anterior–corneal half and posterior-retinal half. Lens, aqueous humor, vitreous humor was separated and intact cornea was carefully obtained without any damage for experiments.

Exposure unit

Typical exposure units for collimated (focussed) and noncollimated (nonfocussed) beam were prepared [Figure 1a and b]. Cornea was exposed to maximum smartphone brightness. The distance between the smartphone and cornea was kept 15 cm.

Permeation study

Permeation of ascorbic acid was measured between the two compartments with the partition of the cornea at room temperature.^[22] Ascorbic acid was loaded in the donor compartment and measured from another compartment (receiver) with respect to time. The donor compartment with the cornea was placed in such a way that it just touched the surface of the saline present in the receiver compartment. The whole set up was kept on the magnetic stirrer with constant stirring to have uniform mixing of the diffused sample in the receiver compartment. After 1 h the sample from the receiver compartment was measured for its absorbance at 265 nm, and the concentration was determined using the standard calibration curve. Percentage permeation was calculated using equation 2.^[22,23]

$$\text{Permeation(\%)} = \frac{\text{Amount of substance permeated in receiver compartment}}{\text{Initial amount in donor compartment}} \times 100 \quad (2)$$

Light transmission study

Light transmission performance of cornea was studied using UV visible detector. The cornea was carefully dissected in a rectangular size and mounted on quartz glass. The mounted cornea was scanned in the closed chamber of UV spectrophotometer in the wavelength range from 400 to 700 nm with an appropriate blank.

Microscopy studies

Bright field, differential interference contrast (DIC) and fluorescence microscopic study: Olympus microscope BX53 was used for imaging. For Bright field imaging, the cornea was illuminated by light source and observed under $\times 40$ objective lens. For DIC imaging, Polarizer, Analyzer with Normanski (DIC) prisms were placed in the path of the light and imaged under $\times 40$ objective lens. The cornea was illuminated with the help of the polarized light, allowed to pass through the first DIC prism. Light from the specimen was collected using the second DIC prism and analyzer, and the

image is obtained. For fluorescence imaging, intact eyeballs were incubated with 10 μl of 0.15 mM fluorescein dye for 15 min in dark. Eyeballs (cornea) were covered with a coverslip to obtain a flatter surface. Cornea was illuminated with UV light and observed under $\times 10$ objective lens with FITC filter.

Ultrastructure study: Environmental Scanning Electron Microscopy (ESEM-FEI quanta250) was used for the ultra-structural study of the corneal surface. Cornea samples for control, noncollimated SPLF exposed, collimated SPLF exposed were imaged. The cornea was simply exposed and immediately scanned under ESEM.

RESULTS AND DISCUSSION

Smart phone light fluxes spectrum and absorbed energy analysis

SPLF spectral emission was analyzed using UV visible detector system. The emission peaks were found at 380 nm and 420 nm [Figure 1c]. Absorbed energy obtained by dosimeter measurement was 2.82 mWm^{-2} and 1.92 mWm^{-2} in collimated and noncollimated beams, respectively. The emitted radiation peak suggests that the current SPLF spectrum fall in UVA (320–410 nm) region, which has high penetration power in the biological system. This radiation has disadvantages such as reduced melatonin secretion, disturbed circadian rhythm, poor vision, etc.^[24]

Insulin study

Transparency of the lens is associated with the native structure of the crystalline protein, which with time aggregates due to radiation exposure and leads to reduced vision or blindness.^[25] In this study, the effect of SPLF was shown on model protein insulin.

The physiological function of lens crystalline is to transmit light and focus an image on the retina. The transparency of the lens is very important. The transparency malfunction results in visual disorder, specifically cataract formation. The lens anterior is lined with a single layer of epithelial cells. The epithelial cell maintains metabolic activity and undergoes mitosis to produce daughter cells. The differential cell elongated to form long thin, ribbon-like structure. During this process, major intracellular changes occur, including the expression of crystalline proteins followed by organelle degradation.^[25]

The alpha and beta alpha crystalline are the major proteins of the lens. The aggregation/polymerization of lens proteins is responsible for light scattering and opacity of the cataractous lens that results in loss of visual performance. UV irradiation is an important cataractogenic factor, the loss of N-terminal extension as a result of mutation/eye lens aging increases the probability of UV induced beta crystalline aggregation.^[26] It has been reported that UV irradiation of beta crystalline causes a change in charge of the protein molecule, the loss of their dimension, structure, and formation of crossed linked protein and oxidation of methionine and tryptophan residues.^[25-27] Muranov *et al.* have shown the dose-dependent aggregation

of the β -crystalline protein where protein aggregation and misfolding contribute largely to the cataract formation.^[28] Destabilization of protein is responsible for partially unfolded and aggregation intermediates, which lead to the formation of insoluble light scattering protein aggregate.^[25]

Therefore in the present study, insulin is used as a model protein to study the effect of SPLF on it. Insulin is a two-chain polypeptide hormone (51 residues) hormone secreted by the β cells of pancreatic islets. Two chains α and β are joined by two interchain disulphide bonds, and α chain contains one intrachain disulfide bonds. It largely consists of an α helical structure. Insulin exists as a mixture of hexameric, dimeric, and monomeric states in solution. The different oligomeric forms of the structure have a critical dependence on its environmental condition.^[29] In this study, the protein was dissolved in 20% acetic acid in order to make sure the protein retains its monomeric form and created a possibility of understanding the effect of smartphone display radiation (SPLF) on the monomeric state of the insulin.

Fluorescence study

Fluorescence emission study

The fluorescence emission intensity of nonirradiated (control) and 1 h irradiated (test) insulin samples were measured at 276 nm. Insulin contains tyrosine; therefore, the protein was excited with 276 nm instead of 280 nm. In this study, the fluorescence intensity of the test sample was found to be unexpectedly enhanced upon SPLF exposure as compared to the control sample [Figure 2a]. The previous report on insulin aggregation showed a decrease in fluorescence intensity with increasing concentration of denaturant.^[30] However, in this report, the slight enhancement was observed and thus confirmed the minor structural and conformational changes around the tyrosine molecule taking place without any aggregation during SPLF exposure. The mechanism of formation of insulin aggregates indicated the transition of monomer to expanded monomer,

then to the unfolded insulin and finally aggregates.^[31] On the basis of the result obtained, the monomeric insulin must be unfolding but slow enough to produce any aggregate provided the amount of energy received by it. Other reports on the UV exposure of energy 2.20 Wm^{-2} had shown the formation of aggregates/fibrils due to an interaction between unfolded insulin molecules.^[32] SPLF energy received by the insulin molecule is smaller than the UV energy and thus the resulting small effect but could be significant for denaturation on subsequent exposures.

Resonance light scattering

RLS was performed to understand the effect of SPLF on structural modification of monomeric insulin. It is a technique that allows the detection of aggregation in protein. It is a technique where the RLS intensity increases with the formation of aggregates in the given wavelength range.^[33] As evident in Figure 2b, the SPLF exposed insulin showed a decrease in the RLS signal as compared to the control insulin. This result indicated the molecular changes taking place in the monomeric insulin with no aggregates on SPLF exposure. The production of such RLS spectra can be correlated to the transition of monomeric insulin to the expanded monomeric insulin or unfolded monomeric insulin, which may further undergo into the dimensions of the aggregates upon continuous and regular SPLF exposure.

Time-resolved fluorescence lifetime studies

Time-resolved fluorescence decay measurements were employed to understand the structural modification and denaturation of the insulin molecule on SPLF exposure. It is a technique in which the measurements of the arrival times of a single photon are detected with respect to the reference signal. TCSPC is a statistical method that requires a high repetitive light source to accumulate a sufficient number of photon events for a required statistical data precision.^[34] Using TCSPC data, the denaturation of the insulin molecule

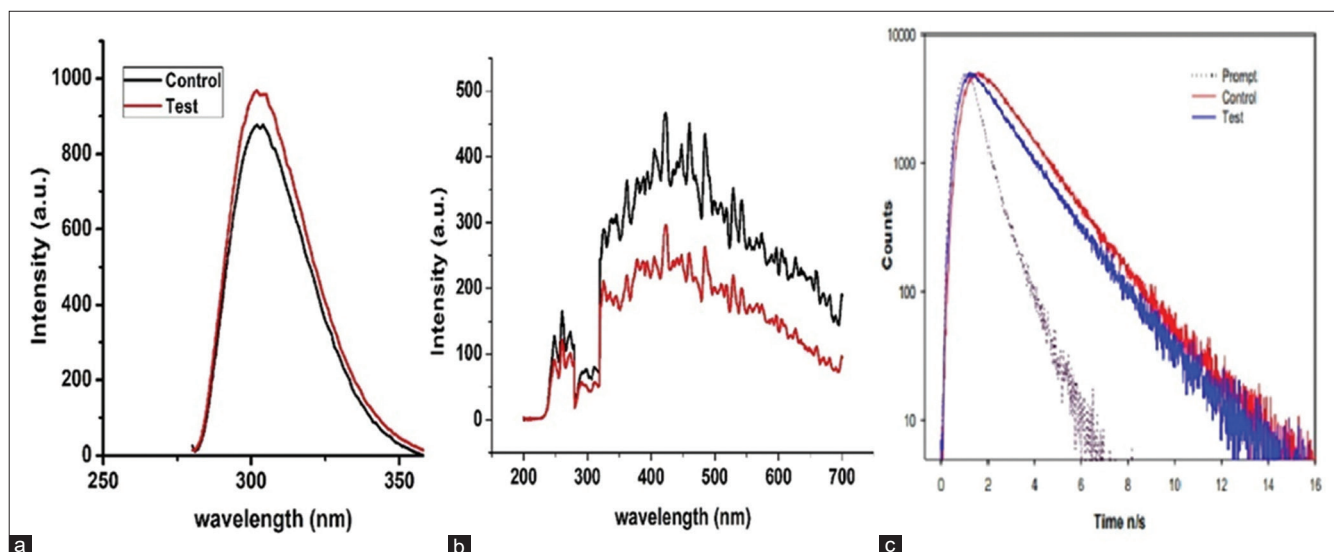


Figure 2: (a) Fluorescence spectra (b) resonance light scattering and (c) Time resolver fluorescence of control and exposed insulin

can be clearly seen from the present study [Figure 2c]. The slight modification in the fluorescence decay of the exposed insulin molecule indicated the conformational changes taking place around the buried tyrosine moieties. As compared to the control, the TSCPC signal of the test insulin sample was found to be decreased. Various reports signify that the time-resolved fluorescence lifetime may increase or decrease upon denaturation. Other reports indicate the increase in the fluorescence lifetime on fibrillation.^[35]

Zeta potential

Zeta potential is a measure of the stability of the colloidal dispersion. The stability of any protein is of prime importance as it is related to its structure and function. Theoretically, it is an electrical potential that is formed between the interface of slipping plane and bulk fluid. The magnitude of the zeta potential determines the fate of the particles. Higher magnitude of zeta potential value does not allow the molecules to come together and flocculate due to the repulsive interaction between them, thus considered to be highly stable. A control sample of insulin was found to have a zeta potential value of +14.2 mV. Zeta potential value decreased to 2.78 mV when insulin sample was exposed to the SPLF. This indicated the effect of exposure on the insulin molecule. Decrease in the zeta potential value indicated that the SPLF exposure created a suitable environment for the transition state that could occur between native and folded insulin protein samples.

Corneal study

Bio-molecular permeation

Amount of ascorbic acid permeated across cornea was calculated as percentage permeation for both collimated and noncollimated SPLF exposure. The percentage permeation was reduced for collimated (focussed) and noncollimated (non-focussed) beam, as shown in Table 1. Which indicates the % permeation of exposed cornea considering control as 100%.

Diffusion of molecules is a fundamental physiological phenomenon which takes place at cellular, tissue, and organ level. The change in flux of these components provides the fundamental properties of the given membrane. There are two pathways for the movement of compound through corneal tissues, namely transcellular and paracellular. In transcellular diffusion, the movement of the compound involves the

cell/tissue partitioning/diffusion, channels diffusion, and carrier-mediated transport. However, in paracellular process, diffusive and convective transport occurs through intracellular spaces and tight junctions.^[36]

Small molecules (water, methanol, ethanol, etc.) readily traverse through cornea. Their permeability constant is very large. In the present investigation, the amount of ascorbic acid permeation was significantly reduced in the collimated display beam, which indicated fundamental modification in the corneal property. The previous report indicated that exposure of UVA increased the stiffness of cornea and modification in the collagen network of the cornea.^[37] Therefore there could be possible changes in the corneal membrane after SPLF exposure.

Light transmission performance

Percentage transmittance (%T) of the collimated and noncollimated beam with respect to control was calculated at Scotopic vision (505 nm).^[38] The experimental condition was dark. Percentage transmittance (%T) (converted to 100% for control) is calculated, and the observed values are given in Table 1. The SPLF exposed cornea showed an increase in absorption of light and less transmittance as compared to control.

Transparency of the cornea has been attributed to the proper molecular arrangement of three layers (epithelium, stroma, and endothelium) and its components.^[39] Furthermore, corneal transparency is related to the hydration level of the corneal stroma. Corneal epithelium and endothelium maintain this hydration level through their active ion transport channel. Perturbation to these cells damage the transport channel and affects the hydration level. Increase or decrease in the hydration level can lead to corneal opacity.^[40] Loss of epithelium layer, damaged keratocytes due to UV radiation, was efficient in inducing corneal opacity.^[18,41] The change in % transmittance indicated greater reduction in % transmittance for collimated exposure than noncollimated exposure. Percentage transmittance indicated that SPLF exposure in dark leads to greater opacity of cornea. Thus, it can be concluded that the high absorption of SPLF in dark could be a reason for the modification of corneal opacity.

Bright field and fluorescence imaging

Bright-field images [Figure 3-top panel] of control corneal epithelial cells showed a regular pattern of epithelial cells, while SPLF exposed cornea showed disturbances in the regular arrangement of epithelial cells. The extent of the disturbance was found to be dependent on the type of SPLF, i.e., collimated/non-collimated beam. A similar pattern of the corneal epithelial cell was reported using AFM and Multimodal Nonlinear Imaging.^[42-44] Bormusov *et al.* showed the loss of cells from the epithelium surface of the lens due to high-frequency exposure of microwave radiation.^[45]

Fluorescence microscopy study showed corneal epithelial cell modifications upon SPLF exposure [Figure 3-bottom

Table 1: Percentage permeation and percentage transmittance of cornea exposed to smartphone light fluxes

SPLF type	Ascorbic acid permeation (%)	Transmittance (%) (505 nm)
Noncollimation beam	77.72±11.23*	67.96±15.88*
Collimation beam	69.35±8.159*,#	49.19±10.02*,#

The results are expressed as mean±SD, * $P < 0.05$ indicates the significant difference between control and exposed cornea. # $P < 0.05$ indicates the significant difference between collimated and noncollimated exposed cornea. $n=7$, statistical paired t -test was used. Control was set as 100%. SD: Standard deviation, SPLF: Smartphone light fluxes

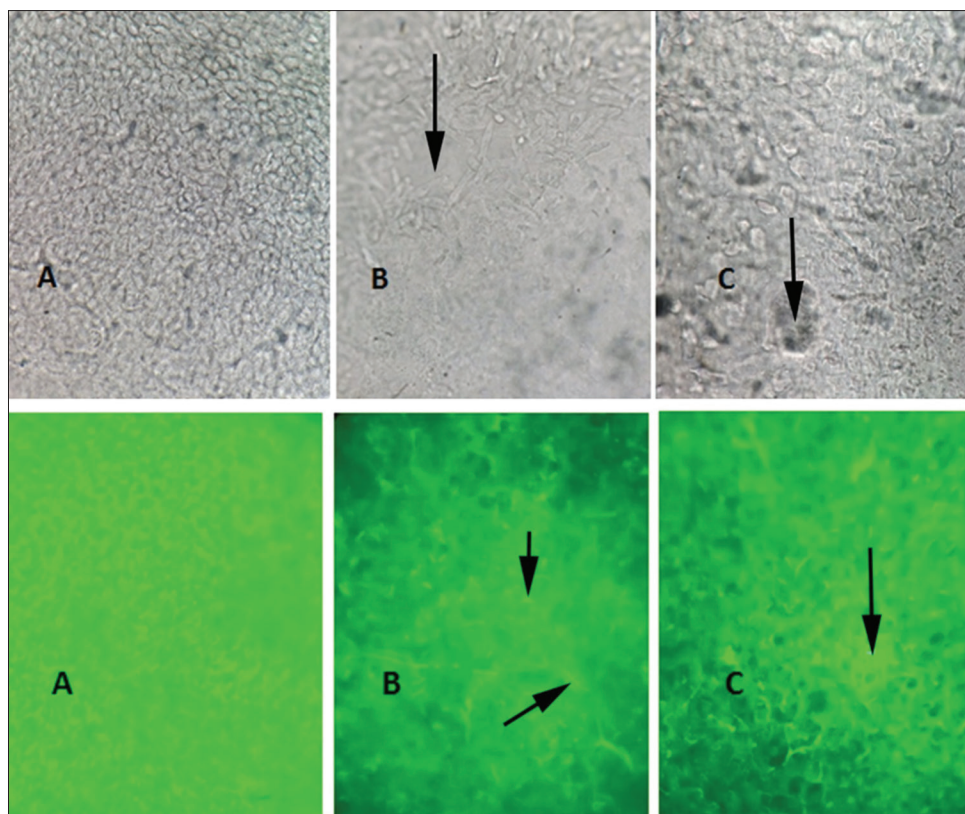


Figure 3: Bright field (top row) and fluorescein stain images of cornea (bottom row): (A) control (B) exposed with noncollimated smartphone light fluxes (arrow indicates exposed intercellular spaces) (C) exposed with collimated smart phone light fluxes (arrow indicates punctate spot)

panel]. Fluorescein dye was used, and it appeared to be penetrating most of the exposed epithelial cell. The area of more intense fluorescence location appeared to indicate fluorescent punctuate spot.^[46-48] The intense fluorescent of the punctuate spot was appeared in spaces between epithelial cells. The relative changes in fluorescent images suggest irregular arrangement/disorganization of the epithelial layer due to exposure.

Differential interference contrast imaging and ultra structure study

Figure 4 (top panel) depicts DIC images of SPLF exposed and unexposed corneal epithelial cells. There are changes in the color and the intensity of exposed and control corneal samples. DIC microscopy is used for cellular/tissue investigation that produces 3D images of unstained cells and tissues. However, results obtained here were due to the difference in refractive index within or between specimen and medium.^[49,50] Changes in the color and the intensity of the DIC images provide a clear indication of the changes in the refractive index of the exposed cornea, which could be due to cellular disturbance/disorganization. The relative change in color and intensity in the images are related to the rate of change of the refractive index.

Ultrastructure study of the cornea was performed using ESEM [Figure 4-bottom panel]. The normal images of the epithelial cell were seen with flat cell surfaces covered

microvilli and the proper gap between two cells. SPLF exposed cells surface were loosened/removed, disruption of intracellular loss/attachment, exposed second and third layer of cells. The normal cell surface was appeared to be lost. The complete loss of the epithelium surface was observed in the collimated display beam, and the collagen fibers were exposed.

With the help of ESEM, the complete loss of epithelium surface was observed and the collagen fibers were exposed due to an intense collimated beam of SPLF. These interwoven collagen fibrils are the composition of Bowman's layer, the immediate layer after the epithelium layer of the cornea. Previous report on cell damage induced by UVA (340–400 nm) irradiation was studied using electron microscopy.^[51]

CONCLUSIONS

It is clear from the experimental data that constant exposure of SPLF damages cornea. Microscopic investigation suggests the degeneration of corneal epithelium cell, which drastically changed the biophysical properties of cornea, such as diffusion, permeability, and refractive index. These disturbances in the fundamental properties have perturbed light transmission performance. In addition, light fluxes from smartphones emit UVA radiation, which has a high penetration power in a biological system. Therefore these UVA can interact with lens protein and may promote protein structure deformation as the optical property of lens proteins (crystalline) depends

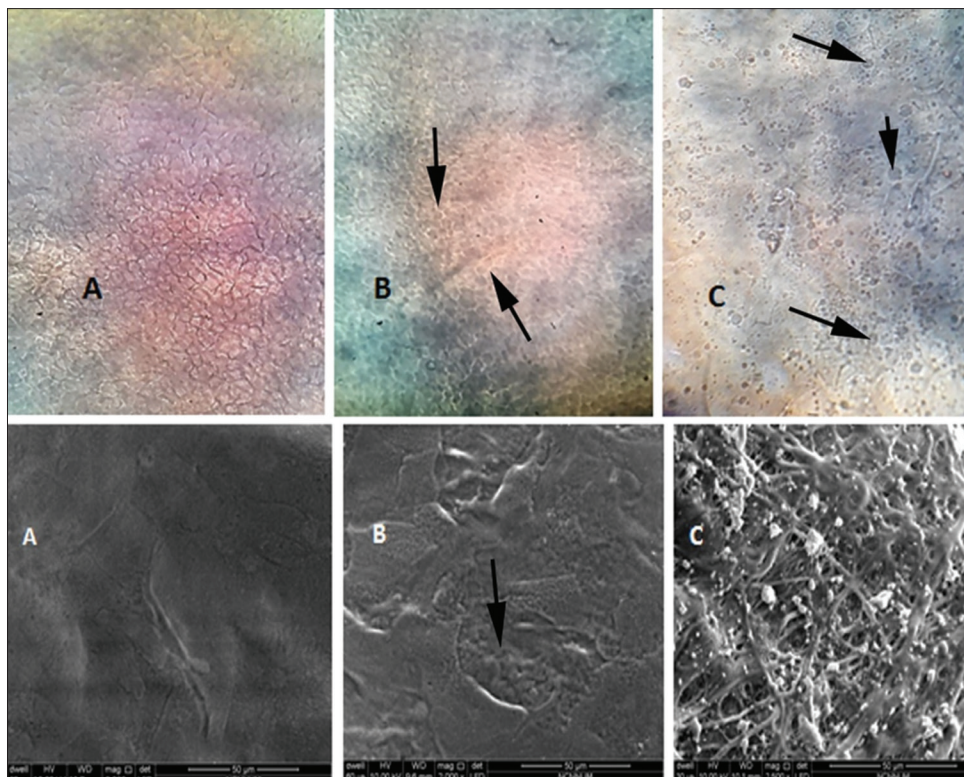


Figure 4: Differential interference contrast (top row) and ESEM images of cornea (bottom row): (A) Control (B) Exposed with noncollimated smartphone light fluxes (arrow indicates exposed intercellular spaces) (C) Exposed with collimated smartphone light fluxes (arrow indicates punctate spot)

on the fine arrangement of their three dimensional structure and hydration. The experimental section (insulin study) has shown the initial level of structural damage and instability in model protein insulin upon SPLF exposure. This loss of native structure may accumulate over time and may interfere with the visual path.

This is a simple study demonstrating the possible impact of SPLF on the visual organ. However, we may able to get deep understanding after observations obtained through various experimental modes (*vitro/vivo*).

Acknowledgments

Authors gratefully acknowledge the Department of Science and Technology, New Delhi under PURSE Scheme to the University of Mumbai, Mumbai, for financial support.

Compliance with ethical standards

The experiments were conducted as per ethical guideline.

Financial support and sponsorship

This study was funded by DST PURSE (UDC/1147-F/2016).

Conflicts of interest

There are no conflicts of interest.

REFERENCES

- Hermann DM, Hossmann KA. Neurological effects of microwave exposure related to mobile communication. *J Neurol Sci* 1997;152:1-4.
- Mora R, Crippa B, Mora F, Dellepiana M. A study of the effects of cellular telephone microwave radiation on the auditory system in healthy man. *ENT-Ear, Nose Throat J* 2006;160:162-3.
- Weisbrot D, Lin H, Ye L, Blank M, Goodman R. Effects of mobile phone radiation on reproduction and development in *Drosophila melanogaster*. *J Cell Biochem* 2003;89:48-55.
- de Gruijl FR, van Kranen HJ, Mullenders LH. UV-induced DNA damage, repair, mutations and oncogenic pathways in skin cancer. *J Photochem Photobiol B* 2001;63:19-27.
- Black HS, deGruijl FR, Forbes PD, Cleaver JE, Ananthaswamy HN, deFabo EC, *et al.* Photocarcinogenesis: An overview. *J Photochem Photobiol B* 1997;40:29-47.
- Schwarz T. Photoimmunosuppression. *Photodermatol Photoimmunol Photomed* 2002;18:141-5.
- Rittié L, Fisher GJ. UV-light-induced signal cascades and skin aging. *Ageing Res Rev* 2002;1:705-20.
- Fisher GJ, Wang ZQ, Datta SC, Varani J, Kang S, Voorhees JJ. Pathophysiology of premature skin aging induced by ultraviolet light. *N Engl J Med* 1997;337:1419-28.
- Ayala MN, Michael R, Söderberg PG. Influence of exposure time for UV radiation-induced cataract. *Invest Ophthalmol Vis Sci* 2000;41:3539-43.
- Moran DJ, Hollows FC. Pterygium and ultraviolet radiation: A positive correlation. *Br J Ophthalmol* 1984;68:343-6.
- Cullen AP. Photokeratitis and other phototoxic effects on the cornea and conjunctiva. *Int J Toxicol* 2002;21:455-64.
- Ravanat JL, Douki T, Cadet J. Direct and indirect effects of UV radiation on DNA and its components. *J Photochem Photobiol B* 2001;63:88-102.
- Obe G, Pfeiffer P, Savage JR, Johannes C, Goedecke W, Jeppesen P, *et al.* Chromosomal aberrations: Formation, identification and distribution. *Mutat Res* 2002;504:17-36.
- Urushibara A, Kodama S, Yokoya A. Induction of genetic instability by transfer of a UVA irradiated chromosome. *Mutat Res* 2014;766:29-34.
- Zimmermann DR, Trüb B, Winterhalter KH, Witmer R, Fischer RW. Type VI collagen is a major component of the human cornea. *FEBS Lett* 1986;197:55-8.
- Meek KM, Knupp C. Corneal structure and transparency. *Prog Retin Eye Res* 2015;49:1-6.

17. Delic NC, Lyons JG, Di Girolamo N, Halliday GM. Damaging effects of ultraviolet radiation on the cornea. *Photochem Photobiol* 2017;93:920-9.
18. Newkirk KM, Chandler HL, Parent AE, Young DC, Colitz CM, Wilkie DA, *et al.* Ultraviolet radiation-induced corneal degeneration in 129 mice. *Toxicol Pathol* 2007;35:819-26.
19. Klan P, Wirz J. *Photochemistry of organic compounds: From concepts to practice.* Wiley 2009;7:112-4.
20. Hatchard CG, Parkar CA. A new sensitive chemical actinometer. II. Potassium ferrioxalate as a standard chemical actinometer *Proc Roy Soc A* 1956;235:518-36.
21. Jaiswal V, Samant M, Kadir A, Chaturvedi K, Nawale AB, Mathe VL, *et al.* UV radiation protection by thermal plasma synthesized zinc oxide nanosheets. *J Inorg Organomet Polym* 2017;27:1211-9.
22. Mohanty B, Mishra SK, Majumdar DK. Effect of formulation factors on *in vitro* transcorneal permeation of voriconazole from aqueous drops. *J Adv Pharm Technol Res* 2013;4:210-6.
23. Singla S, Majumdar DK, Goyal S, Khilnani G. Evidence of carrier mediated transport of ascorbic acid through mammalian cornea. *Saudi Pharm J* 2011;19:165-70.
24. Gomes C, Preto S. Blue light: A blessing or a curse? *Procedia Manuf* 2015;3:4472-9.
25. Moreau KL, King JA. Protein misfolding and aggregation in cataract disease and prospects for prevention. *Trends Mol Med* 2012;18:273-82.
26. Sergeev YV, Hejtmancik JF, Wingfield PT. Energetics of domain-domain interactions and entropy driven association of beta-crystallins. *Biochemistry* 2004;43:415-24.
27. Andley UP, Clark BA. The effects of near UV radiation on human lens β crystallins: Protein structural changes and the production of O₂ and H₂O₂. *Photochem Photobiol* 1989;50:97-105.
28. Muranov KO, Maloletkina OI, Poliansky NB, Markossian KA, Kleymenov SY, Rozhkov SP, *et al.* Mechanism of aggregation of UV-irradiated β L-crystallin. *Exp Eye Res* 2012;92:76-86.
29. Ahmad A, Uversky VN, Hong D, Fink AL. Early event in the fibrillation of monomeric insulin. *J Biol Chem* 2005;30, 280:42669-75.
30. Bekard IB, Dunstan DE. Tyrosine autofluorescence as a measure of bovine insulin fibrillation. *Biophys J* 2009;97:2521-31.
31. Ahmad A, Millett IS, Doniach S, Uversky VN, Fink AL. Partially folded intermediates in insulin fibrillation. *Biochemistry* 2003;42:11404-16.
32. Correia M, Neves-Petersen MT, Jeppesen PB, Gregersen S, Petersen SB. UV-light exposure of insulin: Pharmaceutical implications upon covalent insulin dityrosine dimerization and disulphide bond photolysis. *PLoS One* 2012;7:e50733.
33. Mariam J, Dongre PM, Kothari DC. Study of interaction of silver nanoparticles with bovine serum albumin using fluorescence spectroscopy. *J Fluoresc* 2011;21:2193-9.
34. Kumaran R, Ramamurthy P. Denaturation mechanism of BSA by urea derivatives: Evidence for hydrogen-bonding mode from fluorescence tools. *J Fluoresc* 2011;21:1499-508.
35. Mudliar NH, Pettiwala AM, Awasthi AA, Singh PK. On the molecular form of amyloid marker, Auramine O, in human insulin fibrils. *J Phys Chem B* 2016;120:12474-85.
36. Malhotra M, Majumdar DK. Permeation through cornea. *Indian J Exp Biol* 2001;39:11-24.
37. Stewart JM, Lee OT, Wong FF, Schultz DS, Lamy R. Cross-linking with ultraviolet-a and riboflavin reduces corneal permeability. *Invest Ophthalmol Vis Sci* 2011;52:9275-8.
38. Russell KH, Bradley JR. *Intermediate Physics for Medicine and Biology.* 4th ed. New York: Springer; 2007. p. 187.
39. Hassell JR, Birk DE. The molecular basis of corneal transparency. *Exp Eye Res* 2010;91:326-35.
40. Edelhauser HF. The balance between corneal transparency and edema: The proctor lecture. *Invest Ophthalmol Vis Sci* 2006;47:1754-67.
41. Pitts DG, Cullen AP, Hacker PD. Ocular effects of ultraviolet radiation from 295 to 365 nm. *Invest Ophthalmol Vis Sci* 1977;16:932-9.
42. Mokhtarzadeh M, Casey R, Glasgow BJ. Fluorescein punctate staining traced to superficial corneal epithelial cells by impression cytology and confocal microscopy. *Invest Ophthalmol Vis Sci* 2011;52:2127-35.
43. Tsilimbaris MK, Lesniewska E, Lydataki S, Le Grimellec C, Goudonnet JP, Pallikaris IG. The use of atomic force microscopy for the observation of corneal epithelium surface. *Invest Ophthalmol Vis Sci* 2000;41:680-6.
44. Aptel F, Olivier N, Deniset-Besseau A, Legeais JM, Plamann K, Schanne-Klein MC, *et al.* Multimodal nonlinear imaging of the human cornea. *Invest Ophthalmol Vis Sci* 2010;51:2459-65.
45. Bormusov E, P Andley U, Sharon N, Schächter L, Lahav A, Dovrat A. Non-thermal electromagnetic radiation damage to lens epithelium. *Open Ophthalmol J* 2008;2:102-6.
46. Fonn D, Peterson R, Woods C. Corneal staining as a response to contact lens wear. *Eye Contact Lens* 2010;36:318-21.
47. Wipperman JL, Dorsch JN. Evaluation and management of corneal abrasions. *Am Fam Physician* 2013;87:114-20.
48. Bakkar MM, Hardaker L, March P, Morgan PB, Maldonado-Codina C, Dobson CB. The cellular basis for biocide-induced fluorescein hyperfluorescence in mammalian cell culture. *PLoS One* 2014;9:e84427.
49. Murphy DB. *Fundamentals of light microscopy and electronic imaging.* 1st ed. New York: Wiley 2002. p. 135-73.
50. Lasslett A. *Principles and Applications of Differential Interference Contrast Light Microscopy.* 2006; https://www.Microscopyu.Com/pdfs/Lasslett_Micro_and_Analysis_20-S9.
51. Godar DE, Miller SA, Thomas DP. Immediate and delayed apoptotic cell death mechanisms: UVA versus UVB and UVC radiation. *Cell Death Differ* 1994;1:59-66.